International Journal of Heat and Mass Transfer 179 (2021) 121673

Contents lists available at ScienceDirect

International Journal of Heat and Mass Transfer

journal homepage: www.elsevier.com/locate/hmt

Multiscale modeling of the effective thermal conductivity of 2D woven composites by mechanics of structure genome and neural networks

Xin Liu [a,b,*], Bo Peng [c], Wenbin Yu [d,1]

[a] Department of Industrial, Manufacturing, and Systems Engineering, University of Texas at Arlington, Arlington, TX 76019, United States
[b] Institute for Predictive Performance Methodologies, University of Texas at Arlington Research Institute, Fort Worth, TX 76118, United States
[c] Dassault Systemes Simulia Corp, Johnston, RI 02919, United States
[d] School of Aeronautics and Astronautics, Purdue University, West Lafayette, IN 47907, United States

ARTICLE INFO

Article history:
Received 8 February 2021
Revised 24 June 2021
Accepted 4 July 2021
Available online 16 July 2021

Keywords:
Effective thermal conductivity
Multiscale modeling
Mechanics of structure genome
Woven composites
Neural networks

ABSTRACT

A data-driven multiscale modeling approach is developed to predict the effective thermal conductivity of two-dimensional (2D) woven composites. First, a two-step homogenization approach based on mechanics of structure genome (MSG) is developed to predict effective thermal conductivity. The accuracy and efficiency of the MSG model are compared with the representative volume element (RVE) model based on three-dimensional (3D) finite element analysis (FEA). Then, the simulation data is generated by the MSG model to train neural network models to predict the effective thermal conductivity of three 2D woven composites. The neural network models have mixed input features: continuous input (e.g., fiber volume fraction and yarn geometries) and discrete input (e.g., weave patterns). Moreover, the neural network models are trained with the normalized features to enable reusability. The results show that the developed data-driven models provide an ultra-efficient yet accurate approach for the thermal design and analysis of 2D woven composites.

© 2021 Elsevier Ltd. All rights reserved.

1. Introduction

Woven composites have been widely used in many structures and products, such as fuselage frames [1], electronic devices [2], and medical implant devices [3], thanks to the excellent mechanical performance and lower manufacturing cost. In addition, woven composites have been used in many structures for the thermal protection, where the thermal conductivity plays a critical role. For example, the National Aeronautics and Space Administration (NASA) developed the Woven Thermal Protection Systems (WTPS) for the Extreme Entry Environment Technology [4]. Some experimental studies also showed that steel yarns appear to be suitable for thermal shielding applications, where the thermal conductivity is an important material property to be optimized [5,6]. The tailorable weave patterns provide great design freedom to enhance the thermal performance of woven composite structures [7]. A common approach to predicting the thermal performance of composites is the direct numerical simulation (DNS) based on the finite element (FE) method. However, due to the complex mesostructures of woven composites, a dense mesh is often required to capture the yarn geometries, which makes a FE model become computationally impractical for real engineering design. Therefore, an efficient and accurate multiscale modeling approach, either physics-based or data-driven, is highly sought-after for the evaluation of the thermal performance of woven composites.

In recent years, several numerical homogenization models have been developed to predict both the effective thermal conductivity of composites at the macroscale and the local temperature and heat flux fields at the mesoscale [8–11]. The most popular approach is the representative volume element (RVE) model based on three-dimensional (3D) finite element analysis (FEA) [9]. However, the major obstacle of the RVE model is still the high computational cost. A novel multiscale constitutive modeling approach called mechanics of structure genome (MSG) was developed by Yu in 2016 [12,13], and has been subsequently extended to predict elastic [14], thermoelastic [15], and viscoelastic properties [16] of different woven composites. The MSG-based two-step homogenization approach to predicting mechanical properties has been demonstrated to be many times to orders of magnitude faster than the RVE models while maintaining the same accuracy [14]. The MSG-based homogenization approach is developed based on the variational asymptotic method (VAM) [17]. Although VAM-based

* Corresponding author at: Department of Industrial, Manufacturing, and Systems Engineering, University of Texas at Arlington, Arlington, TX 76019, United States.
E-mail address: xin.liu@uta.edu (X. Liu).

[1] W. Yu is the co-founder and CTO of AnalySwift, a company which might license a version of SwiftComp related with the work presented in this article.

https://doi.org/10.1016/j.ijheatmasstransfer.2021.121673
0017-9310/© 2021 Elsevier Ltd. All rights reserved.

models have been developed to predict the thermal conductivity of unidirectional (UD) fiber-reinforced composites [18,19], there are still several challenges for the woven composites. First, the multiscale modeling of woven composites usually has three scales: microscale (fiber and matrix level), mesoscale (yarn and matrix level), and macroscale (structural level). To predict the effective thermal conductivity of woven composites, features from both the microscale and mesoscale need to be considered. Second, the material orientation varies along the yarn path in woven composites, which should be carefully addressed because the effective thermal conductivity of yarns is often defined in the local material coordinate system [14]. Third, due to the additional computational burden at the mesoscale, the physics-based models usually cannot meet the efficiency requirement for the design optimization, which requires the three-scale modeling to be performed iteratively to find the optimal design parameters.

In this paper, the MSG-based model is extended to solve the first two challenges. The third challenge is solved by developing ultra-efficient data-driven models by artificial neural networks (ANN). The ANN model is an advanced machine learning model that can be used to construct a complex relationship between input features and output results. The ANN models have been successfully employed to solve many computationally expensive multiscale modeling problems [20,21]. For woven composites, features at both the microscale and mesoscale govern the macroscale effective thermal conductivity, and thereby must be considered in the ANN model. In addition, the weave pattern of two-dimensional (2D) woven composites is also an important design parameter. In this paper, three commonly used 2D woven composites (i.e., plain, 2 by 2 twill, and 5 harness satin) are incorporated into the ANN model. Therefore, the ANN models with mixed input, both continuous (e.g., fiber volume fraction and yarn geometry) and discrete (e.g., different weave patterns), are developed.

The remainder of this paper is organized as follows. In Section 2 of the paper, the mathematical framework of the MSG-based thermal conductivity homogenization is derived. Both the microscale and mesoscale homogenization analyses are carried out and compared with 3D RVE models. The accuracy and efficiency of the MSG-based model are detailed discussed. Section 3 first reviews the basis of the ANN model. Then, the training process and the model validation are presented and the results are discussed. Section 4 concludes the paper.

2. Two-step homogenization by the MSG model

2.1. Mathematical framework

Based on the MSG theory, a homogenized model is constructed by minimizing the information loss between the original heterogeneous body and the homogenized body. The information for thermal conduction analysis is the "energy" density of the structure genome (SG) of the original structure [19]. Two coordinate systems are introduced: macro-coordinates x_i and micro-coordinates y_i. The macro-coordinates are used to describe the original structure and the micro-coordinates are used to describe the SG. Because the size of a SG is much smaller than the wavelength of the macroscopic deformation, the two coordinate systems can be related as $y_i = x_i/\varepsilon$ with ε being a small parameter [12,13]. The partial derivative of a function $f(x_k, y_j)$ can be expressed as:

$$\frac{\partial f(x_k, y_j)}{\partial x_i} = \frac{\partial f(x_k, y_j)}{\partial x_i}|_{y_j=\mathrm{const}} + \frac{1}{\varepsilon}\frac{\partial f(x_k, y_j)}{\partial y_i}|_{x_k=\mathrm{const}} \equiv f_{,i} + \frac{1}{\varepsilon} f_{|i} \tag{1}$$

Due to the different thermal conductivities of the constituents in a composite material, the temperature field in a composite material is heterogeneous. One can define this temperature field ϕ as:

$$\phi(x_1, x_2, x_3, y_1, y_2, y_3) = \bar{\phi}(x_1, x_2, x_3) + \varepsilon w(x_1, x_2, x_3, y_1, y_2, y_3) \tag{2}$$

where the $\bar{\phi}$ is the temperature field in the homogenized material and w is the unknown fluctuating function, representing the difference in the temperature fields of the original and homogenized materials. The temperature gradient can be computed as using Eqs. (1) and (2):

$$\phi_{,i} = \frac{\partial \phi}{\partial x_i} = \bar{\phi}_{,i} + \underline{\varepsilon w_{,i}} + w_{|i} = \bar{\phi}_{,i} + w_{|i} \tag{3}$$

The underline term is removed since it contributes negligibly to the total "energy" [17]. The temperature fields in the original and homogenized structures should be equivalent in an average sense. In addition, periodic boundary conditions (PBCs) are applied to the SG. Therefore, the following constraints should be satisfied:

$$\langle \phi \rangle = \bar{\phi} \quad \text{and} \quad \phi^+ = \phi^- \tag{4}$$

where the $\langle \cdot \rangle$ denotes the volume average over the SG. The superscripts + and - denote the quantities on the corresponding periodic boundaries. Eq. (4) implies that the fluctuating functions should follow the following constraints:

$$\langle w \rangle = 0 \quad \text{and} \quad w^+ = w^- \tag{5}$$

The effective conductivity $\bar{K}_{ij}$ can be defined in terms of "energy" integrals [18,22] (Note that this "energy" is different from the free energy defined by thermodynamics):

$$\Pi = \frac{1}{2}\langle \phi_{,i} K_{ij} \phi_{,j} \rangle = \frac{1}{2}\bar{\phi}_{,i}\bar{K}_{ij}\bar{\phi}_{,j} \tag{6}$$

where K_{ij} is the 3 by 3 thermal conductivity of the constituents in composite materials. Plug Eq. (3) into Eq. (6) gives:

$$\Pi = \frac{1}{2}\left\langle \left(\bar{\phi}_{,i} + w_{|i}\right)^T K_{ij}\left(\bar{\phi}_{,j} + w_{|j}\right)\right\rangle \tag{7}$$

The fluctuating function w_i can be solved by taking the variation of Eq. (7). However, most practical engineering problems are 2D or 3D problems, which cannot be easily solved analytically. Thus, the finite element method (FEM) is used to solve a variational statement. The Eq. (7) can be rewritten as:

$$\Pi = \frac{1}{2}\left\langle \left(\nabla\bar{\phi} + \Gamma_h w\right)^T K\left(\nabla\bar{\phi} + \Gamma_h w\right)\right\rangle \tag{8}$$

where ∇ is the gradient operator $\left[\frac{\partial}{\partial y_1} \quad \frac{\partial}{\partial y_2} \quad \frac{\partial}{\partial y_3}\right]$. The Γ_h can be found in Appendix A. The fluctuating functions are represented using shape functions over the SG as:

$$w\left(x_k, y_j\right) = S\left(y_j\right)V(x_k) \tag{9}$$

where S is the standard shape functions depending on the type of elements. V is the nodal values of fluctuating functions to be solved. Substituting Eq. (9) into Eq. (8), the discretized version of the variational statement can be obtained as:

$$\Pi = \frac{1}{2}\left(V^T E V + 2V^T D_{hg}\nabla\bar{\phi} + \nabla\bar{\phi}^T D_{gg}\nabla\bar{\phi}\right) \tag{10}$$

where

$$E = \left\langle (\Gamma_h S)^T K (\Gamma_h S)\right\rangle, \quad D_{hg} = \left\langle (\Gamma_h S)^T K\right\rangle, \quad D_{gg} = \langle K \rangle \tag{11}$$

Performing the variation $\delta\Pi = 0$ subjected to the constraints in Eq. (5), the following system can be obtained:

$$EV = -D_{hg}\nabla\bar{\phi} \tag{12}$$

The solution V can be symbolically expressed as:

$$V = V_0\nabla\bar{\phi} \tag{13}$$

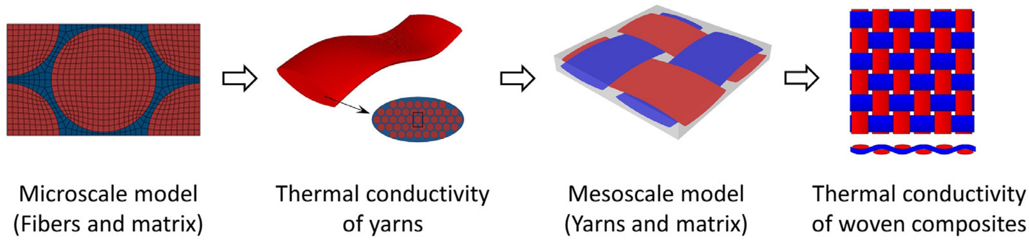

Fig. 1. Two-step homogenization of thermal conductivity of woven composites.

Table 1
Thermal parameters of constituents at room temperature (25 °C) [26].

Thermal conductivity (W m^{-1} K^{-1})	Carbon fiber T700S-12K	Epoxy resin JC-02A
Fiber direction	10.200	0.180
Transverse direction	1.256	0.180

where $V_0 = -E^{-1}D_{hg}$. Plug Eq. (13) into Eq. (10), the "energy" can be expressed as:

$$\Pi = \frac{1}{2}\nabla\bar{\phi}^T\left(V_0^T D_{hg} + D_{gg}\right)\nabla\bar{\phi} \tag{14}$$

where the effective thermal conductivity is $\bar{K} = V_0^T D_{hg} + D_{gg}$. The $\bar{K}$ can be used to perform heat conduction analysis at the macroscale to get the temperature gradient $\nabla\bar{\phi}$ in the homogenized structure, which can be employed to perform dehomogenization analysis to get the local heat flux over the SG. The local fluctuating functions are obtained by:

$$w = SV_0\nabla\bar{\phi} \tag{15}$$

The local temperature gradient over the SG can be subsequently determined by plugging Eq. (15) into Eq. (3):

$$\phi_{,i} = \bar{\phi}_{,j} + \Gamma_h SV_0\bar{\phi}_{,j} \tag{16}$$

The local heat flux within each constituent over the SG can then be computed based on the 3D Fourier constitutive relation [18]:

$$q_i = -K_{ij}\phi_{,i} \tag{17}$$

2.2. Microscale modeling

The two-step multiscale homogenization framework of the effective thermal conductivity of woven composites is illustrated by Fig. 1. The thermal conductivities of fiber and matrix are provided by manufacturers. The effective thermal conductivity of yarns is computed based on a hexagonal-packed micromechanical model. The mesoscale model is composed of yarns and matrix, which computes the effective thermal conductivity of woven composites. All the microscale and mesoscale analyses are performed using a single CPU on the Windows workstation with Intel(R) Core(TM) i7-9750H CPU and 32.0 GB installed memory (RAM). The MSG models are carried out using SwiftComp^{TM} [23] and the RVE models are carried out using commercial FEA software Abaqus [24].

The thermal conductivities of fiber and matrix are listed in Table 1. The 2D SG is used to compute the 3D thermal conductivity of yarns instead of a 3D structure like an RVE as shown in Fig. 2. Note that this is because the SG is the mathematical building block while the RVE is the physical building block [14]. The sizes in Fig. 2 are dimensionless that are just used to describe the selected microstructure. Other microstructures (e.g., square-packed) can also be used in the proposed methodology. The effective thermal conductivities of yarns with different fiber volume fractions are computed by the proposed MSG model and RVE model. The RVE model is solved using the Abaqus micromechanics plugin developed by Dassault Systemes [25]. After the mesh convergence study, a total of 840 4-node quadrilateral elements and 8-node hexahedral elements are used in the MSG model and RVE model respectively.

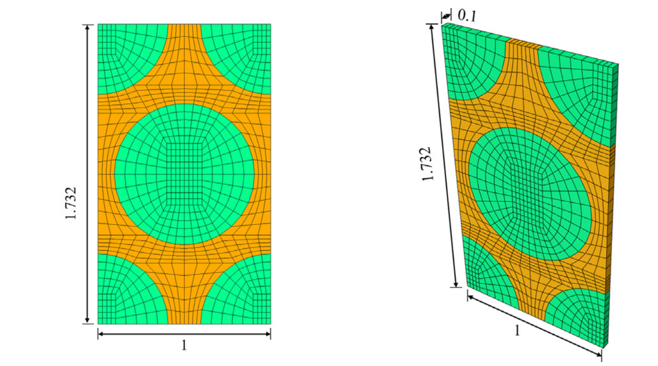

(a) 2D SG (generated by Gmsh[27]) (b) 3D RVE (generated by Abaqus)

Fig. 2. Microscale models for homogenization analysis.

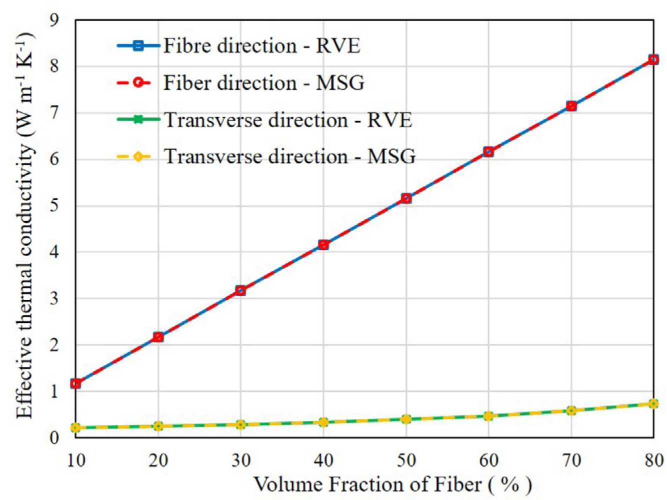

Fig. 3. Effective thermal conductivity of yarns using MSG model and RVE model.

Fig. 3 shows the effective thermal conductivities of yarns in the fiber and transverse directions with different fiber volume fractions. The MSG results show excellent agreement with ones based on the RVE model using 3D FEA. The difference is negligible (the largest one is 0.000012%). For the computing time of one homogenization analysis, the MSG model took 0.063 s while the RVE model took 7.625 s. The significantly improved computational efficiency mainly comes from two parts. First, the SG only uses a 2D structure which has fewer degrees of freedom than the 3D structure in the RVE model. Second, the MSG theory is developed by minimizing the "energy" which only requires solving the system

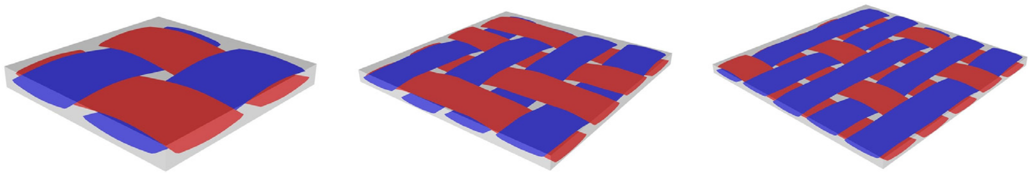

Fig. 4. Three 2D woven composites.

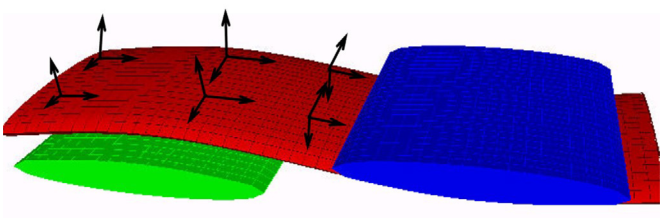

Fig. 5. Material coordinate system varies along the yarn path.

of equations once while the RVE model needs to perform three FE analyses to get the full thermal conductivity matrix.

2.3. Mesoscale modeling

The developed MSG model is further used to predict the effective thermal conductivity of three commonly used 2D woven composites at the mesoscale: plain, 2 by 2 twill (twill), and 5 harness satin (5HS) woven composites (Fig. 4). The effective thermal conductivity of yarns is obtained from the microscale analysis with the fiber volume fraction 60%, which gives $k_{11} = 6.157$ W m^{-1} K^{-1} and $k_{22} = k_{33} = 0.473$ W m^{-1} K^{-1} for the yarns. The yarn spacing is 1 mm, thickness is 0.1 mm, and width is 0.8 mm. The woven composites are generated and meshed using TexGen4SC, which can be freely accessed in the cloud at cdmHUB.org (https://cdmhub.org/resources/texgen4sc) [14,27]. The mesoscale models take the voxel mesh with 32,000 8-node brick elements after a convergence study.

As mentioned in Section 1, the effective thermal conductivity of yarns is obtained in the material coordinate system while the material coordinate system varies along with the yarn path (see Fig. 5). Therefore, the effective thermal conductivity in the global coordinate system needs to be obtained using a direction cosine matrix $\boldsymbol{\beta}$ [14] as:

$$\boldsymbol{K} = \boldsymbol{\beta}^T \boldsymbol{K}' \boldsymbol{\beta} \tag{18}$$

where the $\boldsymbol{K}'$ and $\boldsymbol{K}$ are the thermal conductivity at the material coordinate and global coordinate system respectively. Table 2 shows the effective thermal conductivity of the three 2D woven composites computed based on the MSG model and RVE model. Fig. 6 shows the temperature fluctuations in the twill woven composites when 3 unit temperature gradients are applied respectively in each direction to the SG. Note that the volume average of the temperature fluctuations equals to zero (see Eq. (5)), and therefore the temperature fluctuations are negative on part of the SG. The matrix elements are hidden for a better view of the temperature distribution in yarns. The results show that the MSG model has the same accuracy as the RVE model but the computational costs are significantly reduced. Note that the three 2D woven composites have the in-plane symmetric which means the $k_{11} = k_{22}$.

Table 2
effective thermal conductivity based on MSG model and RVE model.

Weave pattern	plain		twill		5HS	
	MSG	RVE	MSG	RVE	MSG	RVE
k_{11} (W m^{-1} K^{-1})	1.993	1.993	2.099	2.099	2.104	2.104
k_{33} (W m^{-1} K^{-1})	0.337	0.337	0.339	0.339	0.337	0.337
Computing time (s)	3.44	12.00	3.50	12.00	3.46	12.00

3. ANN model for effective thermal conductivity

Although the MSG model shows extraordinary computational efficiency over the RVE model, it is still very expensive for the design optimization of thermal conductivity in woven composites, because iterations of multiscale modeling need to be performed to consider the design parameters across different scales. In addition, many gradient-based optimization algorithms require the model to be differentiable while numerical models usually cannot meet this requirement. Although some analytical models are very efficient and differentiable [7], the ad hoc assumptions hinder the application of these models to general woven composites with arbitrary yarn geometries (e.g., yarn width, thickness, and spacing) and weave patterns. In recent years, ANN models have been increasingly used as surrogate models to provide an ultra-efficient alternative to physics-based models [28–30]. With advanced algorithms and growing training data, ANN models can achieve almost the same accuracy as the physics-based models with the same efficiency as analytical models. In this paper, ANN models with mixed continuous and discrete input will be developed for predicting the thermal conductivity of three 2D woven composites.

3.1. Mathematical framework

The architecture of a feed-forward ANN model is given in Fig. 7. An ANN model contains three different types of layers: input layer, hidden layer(s), and output layer. The units in each layer are called neurons. Each neuron is connected to other neurons in the adjacent layers through weights. A weight parameter w^l_{ji} measures the influence of the ith neuron in the $(l-1)$th layer on the jth neuron in the lth layer. A bias term b^l_j is used in the jth neuron in the lth layer to cover a wider range [31].

The value of a neuron a^l_j is computed by adding the sum of the weighted inputs from the previous layer and a bias:

$$a^l_j = g\left(z^l_j\right) = g\left(\sum_{i=1}^{k} w^l_{ji} a^{l-1}_i + b^l_j\right) \tag{19}$$

where k is the total number of neurons in the $(l-1)$th layer. $g(\cdot)$ is defined as the activation function to capture the nonlinear functions. The Rectified Linear Unit (ReLU) function given in Eq. (20) is used as the activation function in this paper.

$$g(z) = max(0, z) \tag{20}$$

A cost function is defined based on the predicted values and observed values, which are used to update the trainable variables

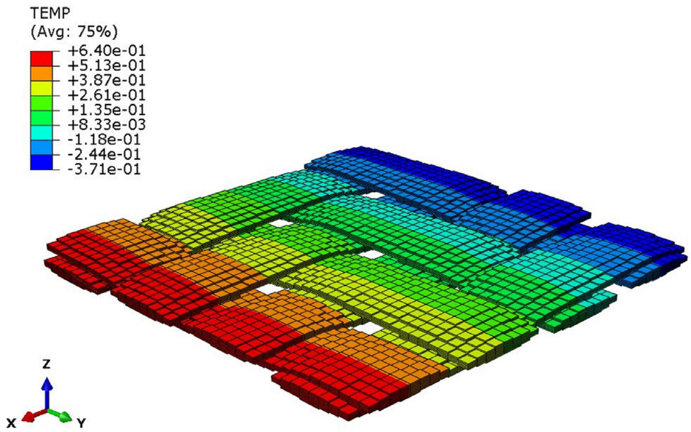

(a) With the x-direction temperature gradient

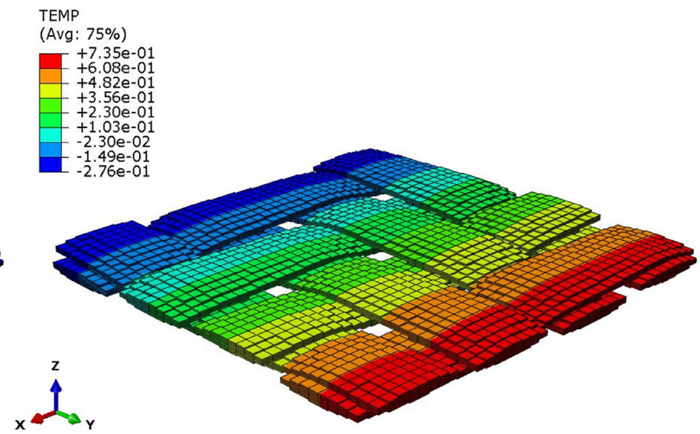

(b) With the y-direction temperature gradient

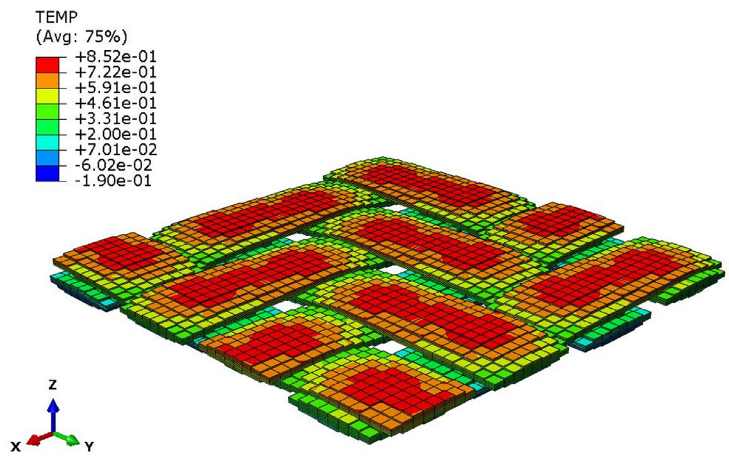

(c) With the z-direction temperature gradient

Fig. 6. Temperature fluctuations in yarns of twill woven composites with PBCs.

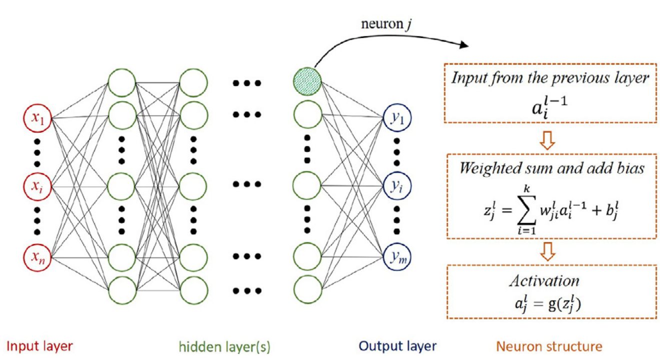

Fig. 7. The architecture of a multilayer feed-forward network.

(i.e., weights and biases) in the ANN model. The cost function is often defined as the mean square error (MSE) [31] in regression problems:

$$L = \frac{1}{2n}\sum^{n}(y - \hat{y})^2 \tag{21}$$

where n is the number of training samples, y is the predicted value from the ANN model and $\hat{y}$ is the labeled output in the training dataset. The weights and biases can be updated using the following equations [32]:

$$w_{ji}^{new} = w_{ji}^{old} - \eta \frac{\partial L}{\partial w_{ji}^{old}} \tag{22}$$

$$b_j^{new} = b_j^{old} - \eta \frac{\partial L}{\partial b_j^{old}} \tag{23}$$

where η is the learning rate. For detailed mathematical background of ANN models and the general applications in composite materials and structures, readers can refer to the references [31,33].

3.2. Training

In this paper, the yarn geometries (i.e., yarn spacing (s_y), thickness (t_y), and width (w_y)) and weave patterns (i.e., plain, twill and 5HS) are the main design parameters of woven composites at the mesoscale. The fiber volume fraction V_f is considered as the design parameter at the microscale. For homogenization analysis, the effective thermal conductivity is associated with a material point at the macroscale, which means the absolute dimensions of yarn geometries are not important. Instead, the relative dimensions such as the ratio of yarn width and spacing $\frac{w_y}{s_y}$ and the ratio of yarn thickness and spacing $\frac{t_y}{s_y}$ can be used as the input for the ANN models. This observation also helps the ANN models to be applied to woven composites with the yarn geometries in different sizes. Moreover, the input dimension of the ANN model is reduced.

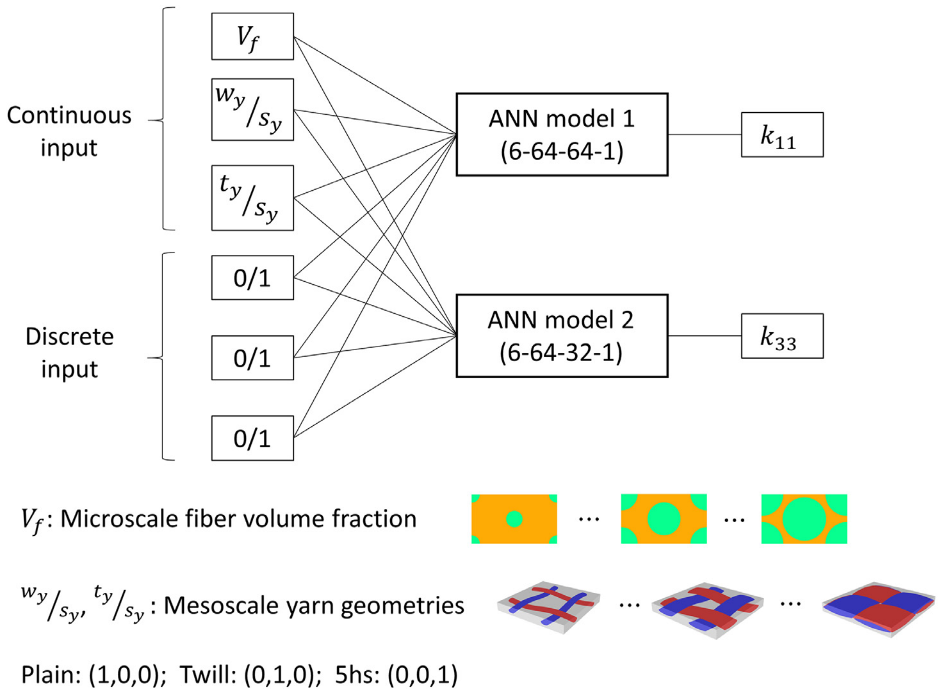

Fig. 8. ANN models for the effective thermal conductivity of 2D woven composites.

Therefore, the continuous input variables in the ANN models in this paper are fiber volume fraction V_f, the ratio of yarn width and spacing $\frac{w_y}{s_y}$, and the ratio of yarn thickness and spacing $\frac{t_y}{s_y}$. The discrete input variables are the three different weave patterns. The one-hot encoding approach is used to convert the discrete input variables into the input of a regression problem [34]. In this problem, there are 3 categories and therefore 3 binary variables are needed. For example, the ANN model of the plain, twill, and 5HS woven composite has the last three input as $[1, 0, 0]$, $[0, 1, 0]$, and $[0, 0, 1]$ respectively. The fiber volume fraction is assumed to vary from 20% to 80%. The ratio of yarn width and spacing $\frac{w_y}{s_y}$ varies from 0.2 to 0.95. The ratio of yarn thickness and spacing $\frac{t_y}{s_y}$ varies from 0.008 to 0.5. These ranges are carefully chosen based on a wide application of woven composites. For example, some thin-ply composites used in the deployable structures only have the $\frac{t_y}{s_y}$ equal to 0.0087 [35]. Fig. 8 shows the input and output data for the two ANN models to be trained.

Two ANN models are trained with the same input variables to predict the in-plane (i.e., $k_{11} = k_{22}$) and out-of-plane (i.e., k_{33}) effective thermal conductivity of 2D woven composites. Although the problem can also be solved by training only one ANN model with two output results, two ANN models will provide the design flexibility when only the in-plane or out-of-plane thermal performance is concerned. In addition, adding another ANN model will not significantly increase the cost of design optimization as the differentiation of ANN models can be very efficient. Therefore, the ANN models to be trained have six-dimensional input and one-dimensional output. The Latin hypercube method [36] is used to sample 8000 datasets for one weave pattern, and therefore 24,000 datasets are generated. 80% of the datasets are used for training and 20% of the datasets are used for testing. After the trial-and-error approach, the ANN model of in-plane thermal conductivity contains 2 hidden layers (64 neurons in layer 1 and 2 respectively), and the ANN model of the out-of-plane thermal conductivity contains 2 hidden layers (64 neurons in layer 1 and 32 neurons in layer 2). The Adam model is used as the optimizer [37].

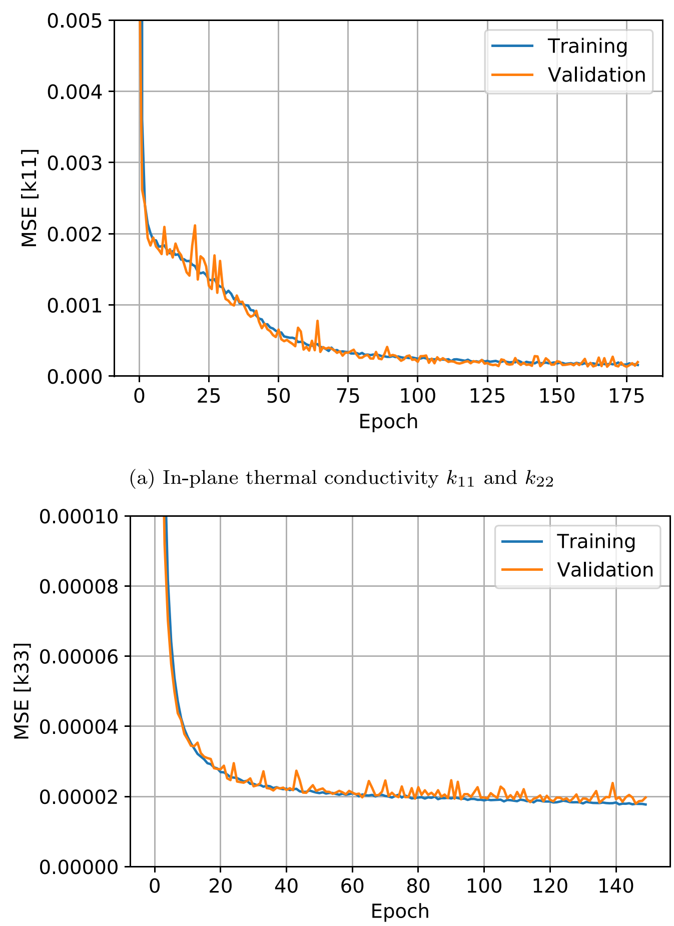

(a) In-plane thermal conductivity k_{11} and k_{22}

(b) Out-of-plane thermal conductivity k_{33}

Fig. 9. Mean squared error during the training.

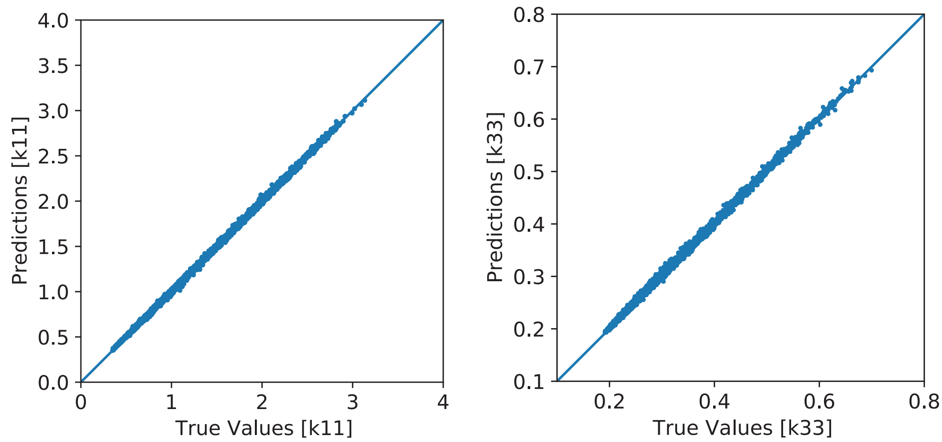

Fig. 10. Comparison of predictions and true values.

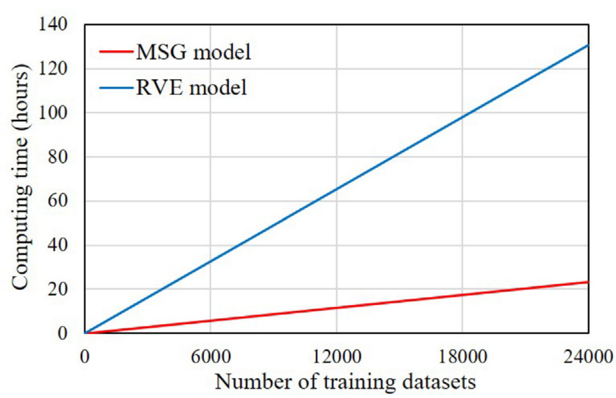

Fig. 11. Comparison of the computing times using MSG model and RVE model.

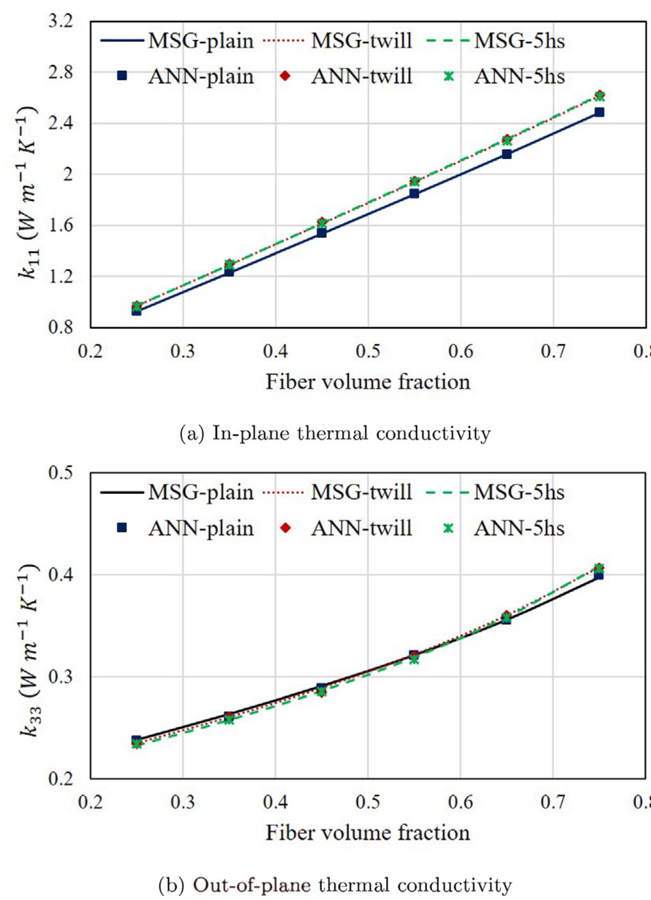

Fig. 12. Comparison of ANN model and MSG model with different fiber volume fractions.

The ANN models are trained using open-source machine learning library Tensorflow [38].

3.3. Validation and discussion

In order to avoid over-fitting, 20% of the training datasets are used to validate the ANN models during the training. As shown in Fig. 9, the variation of the loss with respect to the epoch suggests that there is no over-fitting in the trained models. An epoch is defined as when an entire training dataset is passed forward and backward through the neural network once [21]. Further, the loss in terms of MSE decreases rapidly with the epoch, which means the hyperparameters (e.g., number of layers and neurons) in the ANN models are reasonable.

Fig. 10 shows the comparison between the predictions using the trained ANN models and the true values in the testing datasets. For an ideally trained model (i.e., 100% accuracy), all the dots will overlap with the line. Note that the data in the testing datasets are not used during the training, thereby providing an unbiased evaluation of the performance of the ANN models.

To better understand the performance of the efficiency of the proposed physics-based data-driven approach, the computing time for generating the 24,000 training datasets based on the MSG model and RVE model is given in Fig. 11. Since the same mesh is used in the mesoscale models, the computing times of the mesoscale models are almost the same for the three 2D woven composites (see Table 2). For a single microscale and mesoscale modeling, the total computing times using the MSG model and RVE model are 3.50 s and 19.60 s respectively. All the analyses are performed using a single CPU on the Windows workstation with Intel(R) Core(TM) i7-9750H CPU and 32.0 GB installed memory (RAM).

The accuracy of the trained ANN models are further discussed by changing the continuous input variables and comparing with the corresponding physics-based models. Fig. 12 shows the thermal conductivity in both in-plane and out-of-plane directions in the 2D woven composites in different fiber volume fraction with $\frac{w_y}{s_y} = 0.8$ and $\frac{t_y}{s_y} = 0.1$. The thermal conductivity k_{11} and k_{33} increases with the increasing fiber volume fraction. Moreover, the twill and 5HS

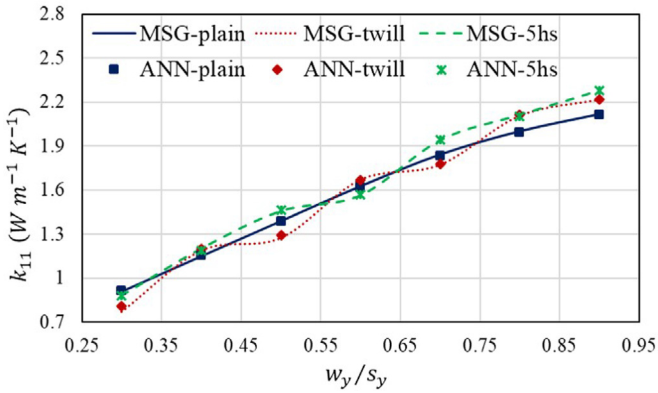

Fig. 13. Comparison of ANN model and MSG model with different $\frac{w_y}{s_y}$ ratios.

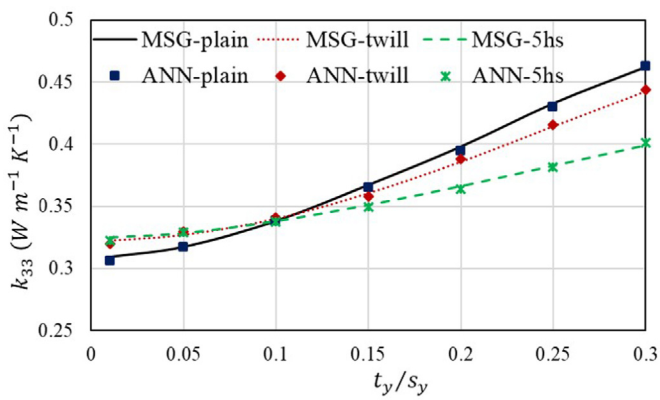

Fig. 14. Comparison of ANN model and MSG model with different $\frac{t_y}{s_y}$ ratios.

woven composites feature a larger in-plane thermal conductivity with the increased fiber volume fraction.

Fig. 13 shows the in-plane thermal conductivity in the 2D woven composites in different ratios of yarn width and spacing with $V_f = 0.6$ and $\frac{t_y}{s_y} = 0.1$. The in-plane thermal conductivity increases with the increasing $\frac{w_y}{s_y}$. In addition, the complex yarn weave patterns in twill and 5HS woven composites lead a non-smooth variation in the thermal conductivity, which usually cannot be well captured by conventional analytical models. Fig. 14 shows the 2D woven composites in different ratios of yarn thickness and spacing with $V_f = 0.6$ and $\frac{w_y}{s_y} = 0.8$. The out-of-plane thermal conductivity increases with the increasing $\frac{t_y}{s_y}$. When the $\frac{t_y}{s_y} = 0.1$, the out-of-plane thermal conductivity in three 2D woven composites are almost the same. When the $\frac{t_y}{s_y} > 0.1$, the plain woven composites show a larger out-of-plane thermal conductivity. Figs. 13 and 14 show the effects of the mesoscale yarn geometries on the thermal conductivity. In reality, the yarn geometries (e.g., weave patterns and cross-sections) are usually very complex that cannot be easily described using a simple function. Although numerical methods with FE mesh can be used to describe complex geometries, a very dense mesh is often required, which could be too computationally expensive for the practical design and analysis. This challenge can be circumvented by developing ultra-efficient data-driven models with almost the same accuracy as the physics-based models. As shown in the Figs. 12, 13, and 14, the trained ANN models show excellent agreement with the MSG models.

4. Conclusions

Physics-based data-driven models were developed to predict the effective thermal conductivity of three commonly used 2D woven composites. The MSG models were developed to perform homogenization analysis of thermal conductivity for woven composites, which capture the complex weave patterns and material orientations along the yarn path. The accuracy and efficiency of the MSG models were compared with the RVE models using 3D FEA for both microscale and mesoscale modeling.

The MSG models provide an efficient high-fidelity multiscale solver to generate training datasets. Two ANN models were developed based on the simulation data to predict the in-plane and out-of-plane thermal conductivity of the 2D woven composites respectively. The ANN models consider both the microscale fiber volume fraction and mesoscale yarn geometries and weave patterns. The input features were mixed with continuous and discrete variables which were solved by the one-hot encoding approach. The fiber volume fraction, yarn geometries, and weave patterns are commonly used as design parameters for 2D woven composite materials. The fiber volume fraction and weave pattern can be directly used as inputs for the proposed ANN models. The yarn geometries can be used to compute the ratios of yarn width/spacing and thickness/spacing as the other inputs for the ANN models. Note that the proposed methodology can be easily adapted to incorporate other weave patterns with complex mesostructures following the same procedure: generate simulation data using MSG, convert weave patterns to ANN inputs by one-hot encoding, and train the ANN model. The trained ANN models in this paper showed excellent agreement with the physics-based model with extraordinary computational efficiency, which can be confidently used in the design and analysis of woven composite structures when thermal performance is concerned.

Declaration of Competing Interest

The authors declare that they have no known competing financial interests or personal relationships that could have appeared to influence the work reported in this paper.

CRediT authorship contribution statement

Xin Liu: Methodology, Conceptualization, Software, Formal analysis, Writing – original draft, Writing – review & editing. **Bo Peng:** Methodology, Software, Formal analysis. **Wenbin Yu:** Writing – review & editing.

Acknowledgement

We would like to thank Composites Design and Manufacturing HUB to provide the online platform so that users can have an easy way to access to our software.

Appendix A. Operator matrix

Γ_h is an operator matrix, and it depends on the dimensionality of the SG. For the 3D SG, Γ_h is defined as:

$$\Gamma_h = \begin{bmatrix} \frac{\partial}{\partial y_1} & 0 & 0 \\ 0 & \frac{\partial}{\partial y_2} & 0 \\ 0 & 0 & \frac{\partial}{\partial y_3} \end{bmatrix} \tag{A.1}$$

For the 2D SG, we just need to vanish the corresponding terms which contain the micro-coordinates that are not used in describing the SG. For the 2D SG, Γ_h is defined as:

$$\Gamma_h = \begin{bmatrix} 0 & 0 & 0 \\ 0 & \frac{\partial}{\partial y_2} & 0 \\ 0 & 0 & \frac{\partial}{\partial y_3} \end{bmatrix} \tag{A.2}$$

References

[1] P. Monnot, J. Lévesque, L.L. Lebel, Automated braiding of a complex aircraft fuselage frame using a non-circular braiding model, Compos. Part A Appl. Sci.Manuf. 102 (2017) 48–63.
[2] F. Tao, X. Lyu, X. Liu, W. Yu, Multiscale analysis of multilayer printed circuit board using mechanics of structure genome, Mech. Adv. Mater. Struct. 28 (8) (2021) 774–783.
[3] Y. Wang, X. Liu, C. Zhu, A. Parsons, J. Liu, S. Huang, I. Ahmed, C. Rudd, N. Sharmin, Production and characterisation of novel phosphate glass fibre yarns, textiles, and textile composites for biomedical applications, J. Mech. Behav. Biomed. Mater. 99 (2019) 47–55.
[4] S.J. Visser, R.J. King, J.M. Thornton, J.M. Brock, N.N. Mansour, Micro-scale artificial weave generation capabilities for thermal protection system material modeling, 11th Ablation Workshop, 2019.
[5] M. Larciprete, Y. Gloy, R.L. Voti, G. Cesarini, G. Leahu, M. Bertolotti, C. Sibilia, Temperature dependent emissivity of different stainless steel textiles in the infrared range, Int. J. Therm. Sci. 113 (2017) 130–135.
[6] M. Larciprete, S. Paoloni, R.L. Voti, Y. Gloy, C. Sibilia, Infrared radiation characterization of several stainless steel textiles in the 3.5–5.1 μm infrared range, Int. J. Therm. Sci. 132 (2018) 168–173.
[7] X.-Y. Zhou, X. Ruan, S. Zhang, W. Xiong, Z. Ullah, Design optimization for thermal conductivity of plain-woven textile composites, Compos. Struct. 255 (2021) 112830.
[8] G. Struzziero, J.J. Teuwen, A. Skordos, Numerical optimisation of thermoset composites manufacturing processes: a review, Compos. Part A Appl. Sci. Manuf. 124 (2019) 105499.
[9] I. Özdemir, W. Brekelmans, M. Geers, Computational homogenization for heat conduction in heterogeneous solids, Int. J. Numer. Methods Eng. 73 (2) (2008) 185–204.
[10] Z. Low, N. Blal, N. Naouar, D. Baillis, Influence of boundary conditions on computation of the effective thermal conductivity of foams, Int. J. Heat Mass Transf. 155 (2020) 119781.
[11] Z. Yang, Y. Sun, J. Cui, Z. Yang, T. Guan, A three-scale homogenization algorithm for coupled conduction-radiation problems in porous materials with multiple configurations, Int. J. Heat Mass Transf. 125 (2018) 1196–1211.
[12] W. Yu, A unified theory for constitutive modeling of composites, J. Mech. Mater. Struct. 11 (4) (2016) 379–411.
[13] W. Yu, Simplified formulation of mechanics of structure genome, AIAA J. 57 (10) (2019) 4201–4209.
[14] X. Liu, K. Rouf, B. Peng, W. Yu, Two-step homogenization of textile composites using mechanics of structure genome, Compos. Struct. 171 (2017) 252–262.
[15] X. Liu, W. Yu, F. Gasco, J. Goodsell, A unified approach for thermoelastic constitutive modeling of composite structures, Compos. Part B Eng. 172 (2019) 649–659.
[16] X. Liu, T. Tang, W. Yu, R.B. Pipes, Multiscale modeling of viscoelastic behaviors of textile composites, Int. J. Eng. Sci. 130 (2018) 175–186.
[17] V. Berdichevsky, Variational Principles of Continuum Mechanics: I. Fundamentals, Springer Science & Business Media, Berlin, 2009.
[18] P. Pitchai, P. Guruprasad, Determination of the influence of interfacial thermal resistance in a three phase composite using variational asymptotic based homogenization method, Int. J. Heat Mass Transf. 155 (2020) 119889.
[19] T. Tang, W. Yu, A variational asymptotic micromechanics model for predicting conductivities of composite materials, J. Mech. Mater. Struct. 2 (9) (2007) 1813–1830.
[20] S. Yan, X. Zou, M. Ilkhani, A. Jones, An efficient multiscale surrogate modelling framework for composite materials considering progressive damage based on artificial neural networks, Compos. Part B Eng. (2020) 108014.
[21] X. Liu, F. Gasco, J. Goodsell, W. Yu, Initial failure strength prediction of woven composites using a new yarn failure criterion constructed by deep learning, Compos. Struct. 230 (2019) 111505.
[22] Z. Hashin, Assessment of the self consistent scheme approximation: conductivity of particulate composites, J Compos Mater 2 (3) (1968) 284–300.
[23] W. Yu, X. Liu, Swiftcomp, 2017,
[24] S.L. Omairey, P.D. Dunning, S. Sriramula, Development of an ABAQUS plugin tool for periodic RVE homogenisation, Eng. Comput. 35 (2) (2019) 567–577.
[25] B. Peng, W. Yu, A micromechanics theory for homogenization and dehomogenization of aperiodic heterogeneous materials, Compos. Struct. 199 (2018) 53–62.
[26] K. Dong, K. Liu, Q. Zhang, B. Gu, B. Sun, Experimental and numerical analyses on the thermal conductive behaviors of carbon fiber/epoxy plain woven composites, Int. J. Heat Mass Transf. 102 (2016) 501–517.
[27] H. Lin, L.P. Brown, A.C. Long, Modelling and simulating textile structures using TexGen, in: Advanced Materials Research, vol. 331, Trans Tech Publ, 2011, pp. 44–47.
[28] Y.M. Seo, K. Luo, M.Y. Ha, Y.G. Park, Direct numerical simulation and artificial neural network modeling of heat transfer characteristics on natural convection with a sinusoidal cylinder in a long rectangular enclosure, Int. J. Heat Mass Transf. 152 (2020) 119564.
[29] X. Liu, F. Tao, W. Yu, A neural network enhanced system for learning nonlinear constitutive law and failure initiation criterion of composites using indirectly measurable data, Compos. Struct. 252 (2020) 112658.
[30] X. Liu, F. Tao, H. Du, W. Yu, K. Xu, Learning nonlinear constitutive laws using neural network models based on indirectly measurable data, J. Appl. Mech. 87 (8) (2020).
[31] M.A. Nielsen, Neural Networks and Deep Learning, Determination press San Francisco, CA, USA:, 2015.
[32] S. Haykin, Neural Networks and Learning Machines, Pearson Education India, 2010.
[33] X. Liu, S. Tian, F. Tao, H. Du, W. Yu, How machine learning can help the design and analysis of composite materials and structures?, arXiv:2010.09438(2020).
[34] A. Géron, Hands-On Machine Learning with Scikit-Learn, Keras, and TensorFlow: Concepts, Tools, and Techniques to Build Intelligent Systems, O'Reilly Media, 2019.
[35] M. Yapa Hamillage, K. Kwok, J.M. Fernandez, Micromechanical modeling of high-strain thin-ply composites, in: AIAA Scitech 2019 Forum, 2019, p. 1751.
[36] J.C. Helton, F.J. Davis, Latin hypercube sampling and the propagation of uncertainty in analyses of complex systems, Reliab. Eng. Syst. Saf. 81 (1) (2003) 23–69.
[37] Z. Zhang, Improved adam optimizer for deep neural networks, in: 2018 IEEE/ACM 26th International Symposium on Quality of Service (IWQoS), IEEE, 2018, pp. 1–2.
[38] M. Abadi, P. Barham, J. Chen, Z. Chen, A. Davis, J. Dean, M. Devin, S. Ghemawat, G. Irving, M. Isard, et al., TensorFlow: a system for large-scale machine learning, in: 12th {USENIX} Symposium on Operating Systems Design and Implementation ({OSDI} 16), 2016, pp. 265–283.